

Energy performance of R22 blended with nanofluids in refrigeration system

S. Vandaarkuzhali^{a,*}, J. F. Xavier^{b,*}, R. Ramadoss^{c,*}, V. Jayaseelan^{d,*},
K. Sudhakar^{e,f,*}

^a*Department of Mechanical Engineering, Mailam Engineering College,
Mailam, 604304, India*

^b*School of Mechanical Engineering, VIT Bhopal University, Bhopal, 466114,
Madhya Pradesh, India*

^c*Department of Mechanical Engineering, Easwari Engineering College, Chennai-
600089, Tamil Nadu, India*

^d*Department of Mechanical Engineering, Prathyusha Engineering College,
Tiruvallur, 602025, Tamil Nadu, India*

^e*Faculty of Mechanical and Automotive Engineering Technology & Automotive
Engineering Centre, Universiti Malaysia Pahang, 26600 Pekan, Pahang,
Malaysia.*

^f*Energy Centre, Maulana Azad National Institute of Technology, Bhopal, 462003,
India*

Nanofluids are possible heat transfer fluids with enhanced thermophysical characteristics and heat transfer performance for improved performance in many devices. The thermal behaviour of air conditioning systems using various nano-fluids is described in this study. The nano-fluid chosen for testing is CuO, ZnO and Al₂O₃, which are combined with the R22 refrigerants with a volume fraction of 0.1 %, 0.3 % and 0.5 % to analyse the air-conditioning Performance. The magnetic stirrer is used to disperse nano-particles and ultrasound for approximately 4 hours, dispersing the specified quantity into compressed oil for 2 hours to the appropriate fraction. The model uses the fluid input information to predict fluid output temperatures, operating pressures, compressor power consumption and overall system output. The experimental results show an increase in performance by using 0.5 percent volume with R22base refrigerant when using CuO.

(Received February 9, 2021; Accepted April 12, 2021)

Keywords: Nano-fluids, Coefficient of Performance, Air conditioning system, Refrigerant, R22

1. Introduction

Due to rapid developments in nanotechnology, new generations of heat transfer fluids are named nanofluids and being developed. The nanoparticle suspended (1-100 nm) have a higher thermal conductivity in traditional fluids compared with base fluid. This principle is used in the suspension of nanoparticles in R22 refrigerants. The efficiency of refrigeration systems, such as home refrigerators and air conditioning, is determined by their physical thermal properties and convective heat transfer nature[1]. Adding nanoparticles to coolant increases coolant transmission and physical thermal properties, thus significantly improving the device performance[2]. Important advances in physical thermal and heat transfer capacities are achieved to increase cooling system efficiency by the use of air conditioning nanoparticles. In a vapour compression cooling system, the lubricant oil in the compressor unit of the system can be supplied with nanoparticles. It is very important to prepare and stabilise the mixture of this lubricant and nanoparticles[3]. Nano lubricants desired to provide stable and robust suspension, lower coagulation and ensured that the prepared nano lubricant did not alter its chemical reaction.

* Corresponding authors: jaiseelanv@gmail.com

Polyalkylene glycol (PAG) [4] is the lubricant oil, a form widely used in cooling and air conditioning systems. This experimental setup uses the standard compressor. No special measures are used to prevent nanoparticles from mixing with coolant since there is a certain amount of lubricating oil in the compressor in a typical air conditioning device that is supplied with coolant. So, in the air conditioning system, a certain volume of lubricating oil circulates along with the refrigerant. The condenser can accumulate lubricating oil if the solubility of the lubricating oil in the refrigerant is poor. If the lubricating oil solubility in the refrigerant is high, the coolant is removed from the compressor by all lubricating oil and there is a chance of abrasion in the compressor. The refrigerant has also combined optimal concentrations of nanoparticles. When the refrigerant is circulated through the compressor, it carries traces of a mixture of lubricant and nanoparticles (nano lubricant) so that the other heat transfer components have a mixture of nano lubricant-refrigerant [5]. Literature has shown proof that the increase in thermal conductivity compared to base liquids in oxide nanoparticles with concentration less than 0.5% Volume. More oxide nanoparticles have a higher concentration and become more insulators. Nanoparticle agglomeration occurs where the percentage is greater than 0.5, leading to a decrease in the heat transfer rate and therefore the concentration of nanoparticles is limited to 0.5 percent [6,7]. The objective of the work is to check the concentration of the three nanofluids in the device and investigate the suction pressure, temperature, discharge pressure and coefficient of performance (COP).

2. Methods and materials

2.1. Characterization of nanoparticles

The Hitachi instrument S-3400 N is used for the surface morphology study and for chemical analysis to scan the SMS microscopy and energy dispersive X-rays analyses (EDXA). The micrographs demonstrated that circular and spherical combinations of aluminium oxides, zinc oxides and copper oxide nanoparticles are shown in Fig. 1, which is less than 100 nm inside nano-area[8]. Nanopowders from aluminium oxide(Al_2O_3), Copper Oxide(CuO) and zinc oxide(ZnO) with a particle size of 50 nm and 99.9% were purchased.

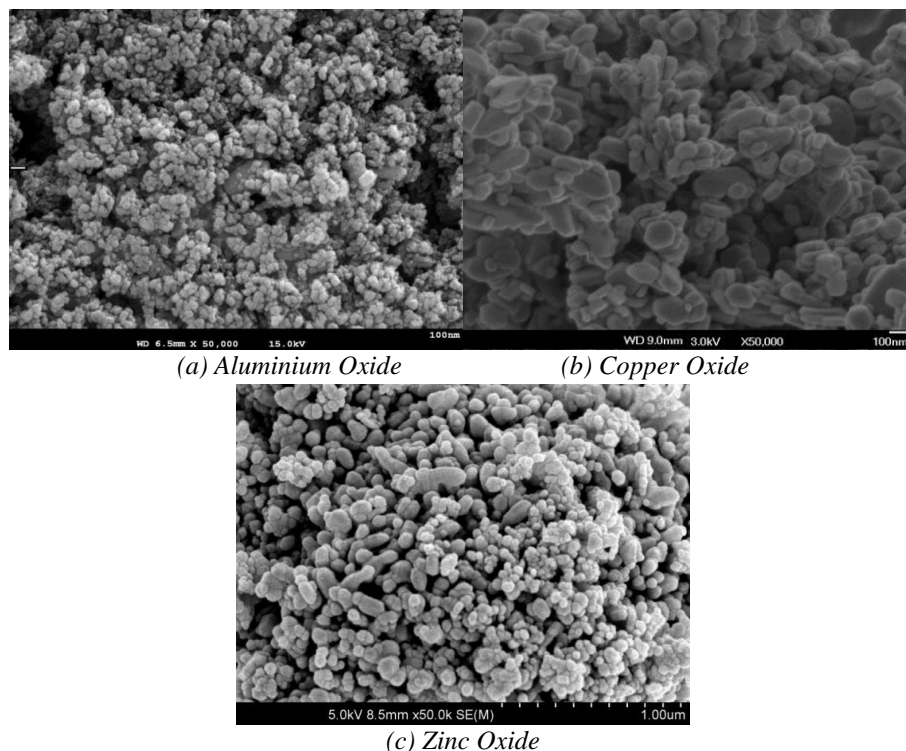


Fig. 1. SEM images of Nano-particles

The pattern of Al_2O_3 nanoparticles in XRD is shown in Fig. 2. Six peaks at the angles of Bragg, at 57.0, 53.8, 44.5, 37.5 and 35.5 were observed in nano $\alpha\text{-Al}_2\text{O}_3$ (50 nm) and 25.0 degradations. Sharp α -alumina peaks are crystalline [9]. The data collected corresponded to the JPDs card file No. 46-1215, confirming the structure of crystalline alumina in the Joint Committee on Card Diffraction Standards (JCPDS).

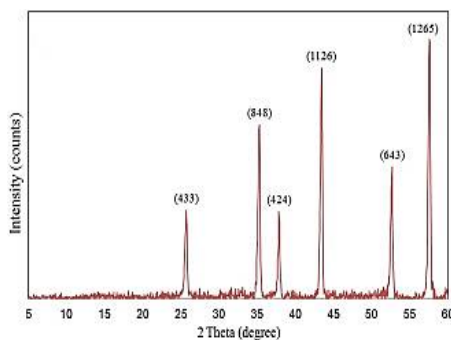


Fig. 2. XRD pattern of Nano Alumina.

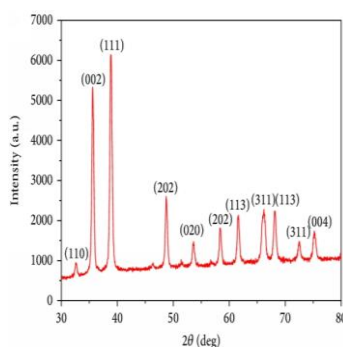


Fig. 3. XRD pattern of Nano Copper oxide.

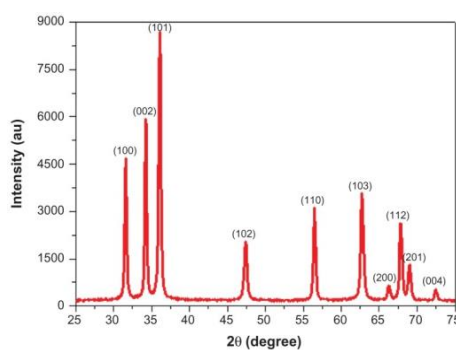


Fig. 4. XRD pattern of Nano Zinc oxide.

The XRD nanoparticles in CuO is shown in Fig. 3. The CuO monoclinic (C_2/c space party, CIPDS card No. 45-0937), is possible to index all the pinnacles in CuO . High-quality nanoparticles of CuO have been prepared and no peaks of any impurities are observed. In XRD patterns and crystallite sizes of less than 100 nm, sharp structural peaks suggest the nanocrystalline nature of CuO nanoparticles. The pattern of zinc oxide nanoparticles in XRD is shown in Fig. 4.

The samples were assigned to (100), (002), (101), (102), (110),(103), (201), (112), (200), and (004) ZnO nanoparticles, with the various peak-like angles of 31.67 °, 34.31 °, 36.14 °, 47.40 °, 56.52 °, 62.73 °, 6.28 °, 67.91 °, 69.03 °, and 72.48 °, suggesting that the samples were polycrystalline, rooted in structure. There have been no characteristic pinnacles of impurities, indicating the synthesization of high-quality ZnO-nanoparticles[10].

The word "top-down" describes processes that create the intended structure employing mechanical or chemical methods, starting from large pieces of material. The top-down proceedings have unrivalled versatility in implementation, given frameworks in a variety of sized systems accessible by mechanical tools or photographic processes. The basic characteristics of top-downs are summarised in Fig. 5.

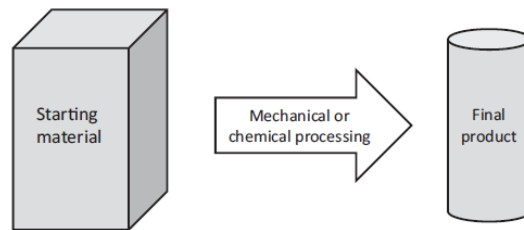


Fig. 5. Conventional products produced by top-down processes.

“Bottom-up” processes typically include chemical processes that include nanoparticles or nano molecules from atoms or molecules, thin films or organized layers as building blocks. These features are often classified as zero, one or two-dimensional nanostructures by using their dimensionality for classification. This is seen in Figure6. This process gives enormous freedom in the composition of the resulting products; however, a comparatively limited number of possible structures are obtained. Processes that are complemented by the self-organization of individual particles create ordered structures. In comparison to the additive technology representing bottom-up processes, top-down techniques are also represented as subtractive technology [11].

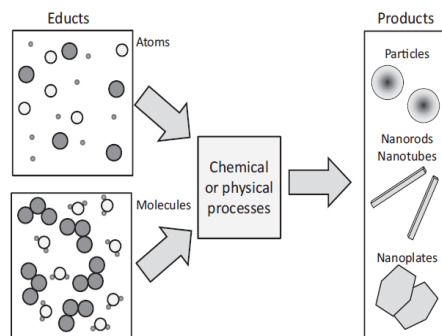


Fig. 6. Chemical synthesis as a bottom-up process.

Fig. 7 demonstrates the description of the nanomaterial synthesis methods at bottom-up and top-down. Nanopowder's powder-based syntheses, amorphous precursor methods, surface techniques (coating and modified nanostructure layers), plastic intensive methods and complicated methods are shown in Fig. 8.

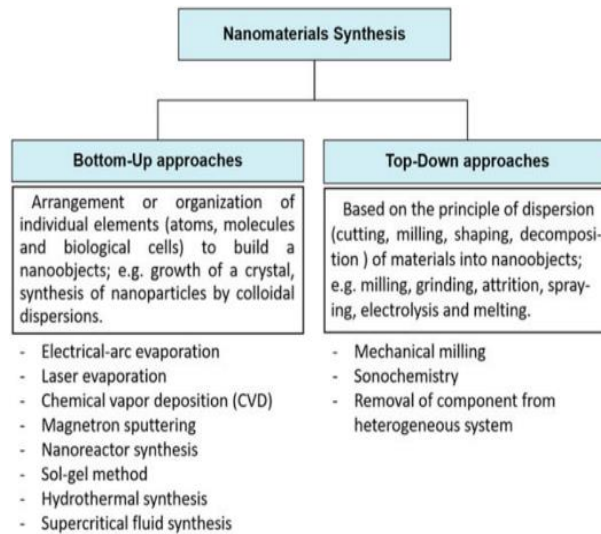


Fig. 7. Methods for the synthesis of Nanomaterials.

Certain methods for generating bulk material nanoparticle are high-energy ball Framing, Mechanochemical Processing, electro-explosion and laser ablation. The approaches to bottom-up include CD-R, CVC, plasma or flame synthesis, laser pyrolysis, precipitation, decreasing, sungel, solvothermal, matrix-mediated (template-assisted) treatment, the assembly itself, etc. The powder method is based upon the development, by compressing powders or alloys with or without other materials and heating polished metals or metal artefacts without melting them thoroughly to reinforce and solidify them. Amorphisation methods in the manufacture of nanomaterials include friction, grinding, pressure and radiation. Compound and intensive methods of plastic deformation are based on different methods for extracting nanomaterials sequentially or simultaneously [12].

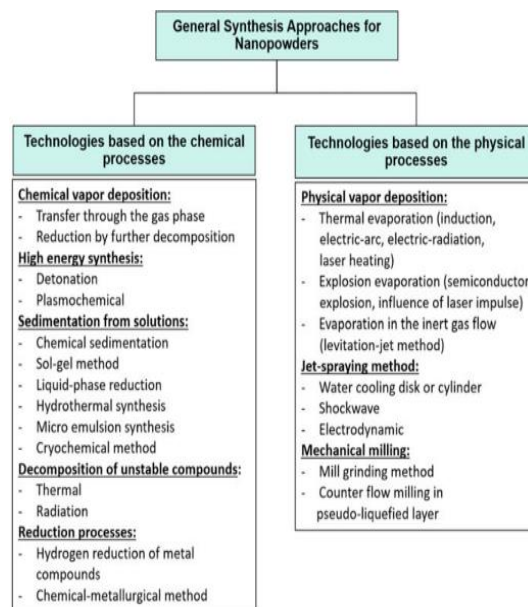


Fig. 8. Nanopowder processing technical processes.

2.2. Synthesis of nanoparticles and nanofluids

Significant improvements in thermal conductivity and heat exchange coefficients with a corresponding increase of energy efficiency are possible at relatively low nanoparticle concentrations. Other factors that affect the efficiency of nanofluids are the substrate, shape and size of nanoparticles, the Zeta potential and pH of the colloidal solution, the type and concentration of the dispersants. Nanofluids in HVAC&R can be used in several ways. It is used in commercial cooling, chiller, and solar panels in absorption systems as secondary fluids. As nanolubricants, they can boost compressor-lubricant thermal dissipation, wear control and intense pressure. Scattering nanoparticles directly in the coolant will enhance the thermodynamic efficiency of cooling machines. The nanofluids also have high thermal conductivity, with Al_2O_3 or CuO increasing 2 to 4 times the base fluid over a small temperature range (20°C to 50°C). Nanofluids are also highly dependent on their temperature. Knowledge of Nanofluids viscosity is necessary if the energy needed to pump fluid through the hydraulic system is to be increased/dismissed. Nanofluids, depending on the concentration and shear stress may be comported like Newtonian or non-Newtonian fluids. Viscosity can also be influenced by the particle size compared to tube size. For the viscosity of the zero shear rate, which rises suddenly above the limit, the dilute limit is recognised. Nanoparticle aggregation greatly increases viscosity. The accurate selection of particulate form, size, material and concentration is generally required to improve the heat transfer in a pressure drop without significant penalization [13].

The nanoparticles mixing still depend on the nanoparticles solvent density and scale. So, the higher is the density of the solvent, the greater the dispersion of nano-articles, the smaller the particle size of the nano-particle. It also depends on the coolant density. A contactless cavitation system for mixing is the best method. Unfortunately, introducing nanoparticles directly to the VCRES framework is not ideal. It is necessary to provide a stable nano-fluid. That is, after a certain time, the nanoparticles should not be dissolved or the nanoparticles in the coolant should be dispersed well. The attainment of nano-refrigerants with a well-dispersed method of nano-fluid preparation only one or two stages. The thermodynamic and mechanical efficiency of cooling machines is improved by nanofluids. The addition of nanoparticles to the operating fluids will greatly increase their transport properties and then their energy efficiency, even if the effect on the pressure drop is thoroughly assessed.

In this analysis, three Nanoparticles, Al_2O_3 , CuO and ZnO are chosen, with a concentration of 0.1%, 0.3% and 0.5%. This is because of its well known thermal characteristics and fast dispersion. Al_2O_3 , CuO and ZnO were directly bought with 50 nm of particulate content, 99.9 percent purity, from the dealer Sigma-Aldrich-Inde. Nanofluids characteristics are 50 nm of particles average size, 3800 kg / m^3 density, 30 W / mK heat-conductivity, 773 J / kgK heat-specific characteristics. A 0.1%, 0.3% and 0.5% are needed for the quantities to be dispersed in compressor oil by magnetic agitators for 2 hours, followed by ultrasound over approximately 4 hours which is shown in Fig. 9. The required quantities can be dispersed by magnetic agitators [14].

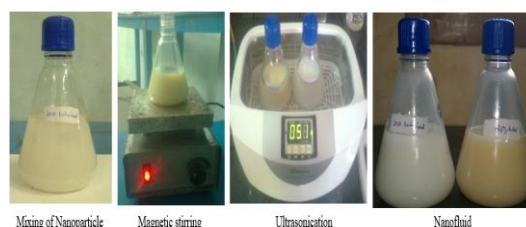


Fig. 9. Synthesis of Nanofluids.

Nanoparticles usually agglomerate, if the base fluid suspends the nanoparticles. The magnetic mixing and subsequent ultrasonic vibration were conducted for 4 hours [10]. All the test samples of Al_2O_3 , ZnO and CuO nanofluids subsequently used in the estimation of their properties were obtained. Ultrasonic vibration (ultrasonic mixing bath) is used to ensure that nanoparticles do

not aggregate with one another. The preparation of the nanofluids samples is for observation purposes and no particulate settling at the base has been observed, even after four hours, of the flask containing CuO, ZnO and Al₂O₃ nanofluids. For cleaning or indirect homogenization of contact, ultrasonic baths may be used. The high-frequency sound wave serves to homogenise the nanoparticles in the lubricant and to evenly agglomerate them [15].

3. Experimental setup

Fig. 10 demonstrates the experimental set-up for the study, which contains a compressor, a condenser fan cooling, an expansion unit and a portion evaporator. As an extension mechanism, the capillary tube is used. Service ports are provided for the air-conditioner inlet and compressor [16]



Fig. 10. Schematic representation of Experimental setup.

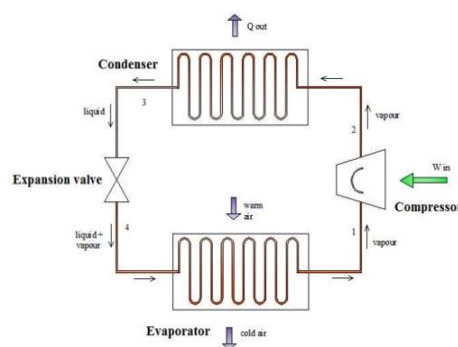


Fig. 11. Vapour compression refrigeration system [17].

Vapour compression cooling systems is shown in Fig. 11. These vapour compression cooling systems are known as generic in vapour cycles, where the coolant (work fluid) is modified during at least one phase. In this method, coolant evaporation takes place at a lower temperature for cooling purposes. For the running of the compressor, mechanical energy is necessary, which is the input of the cooler system.

On a platform at a constant temperature, the experimental setup was mounted. Atmospheric temperatures were 30 °C. There was less than 0.35 m / s of airflow volume. Resistance thermo-couples are used to measure temperature in various parts of the experimental setup. 12 thermocouples were used for experimentation. The pressure is determined by the pressure measuring gauges at the compressor suction, discharge, capacitor exhaust and evaporator exhaust. Digital Watt-hr metre was used to calculate the device energy consumption. This method includes reciprocal compressors used in plants with a capacity of up to 100 tonnes. The total

volume of the gas that is drawn into the cylinders is smaller than the volume displaced in the device for reciprocal compressors, which may be single or multi-cylinder cylinders due to clearing, leaks past pistons and valves and throttling effects on suction and discharge valves. All instruments used have been calibrated and initial tests have been measured at least 5 times, while accuracy and precision have been assured [18]. The current COP is calculated by equation 1.

$$\text{COP} = \text{Cooling load} / \text{Power input} \quad (1)$$

They were dissolved uniformly and not recognisable as a separate entity after nanoparticles were combined with refrigerants. Therefore, nanoparticles are not dynamically noticeable. Suction pressure and suction temperature determined by the experimental method even discharge temperature calculate by the experimental exit flow [19].

4. Result and discussion

4.1. Effect on suction pressure

A pressure drop that develops during the coolant flow is one of the essential parameters for the efficiency of nanofluid usages. The higher density and viscosity of coolants is predicted to fall at higher pressure. This led to the drawbacks of the use of nanofluids as coolant liquids [20]. Pressure drop and pumping capacity have been achieved in a cooling device with nanocolds and nanorefrigerants have a substantially higher thermal conductivity at very low particle levels than typical refrigerants, which is highly dependent on the temperature. This may be considered as one of the key parameters in improving cooling and air conditioning systems efficiency. Increased suction pressure under all conditions as more nanofluids with refrigerant is added. However, the continuous operation of the air conditioning system decreases the suction tension. In refrigerant nano-particles, pressure decreases in the suction head because of the rise in Nano-refrigerant density as shown in Figure 12. For Al_2O_3 , ZnO, and CuO nanoparticle maximum suction pressure is 8.69, 11.16 and 8.89 bar for 0.5%, and minimum 4.83, 7.14 and 4.97 bar for 0.1%.

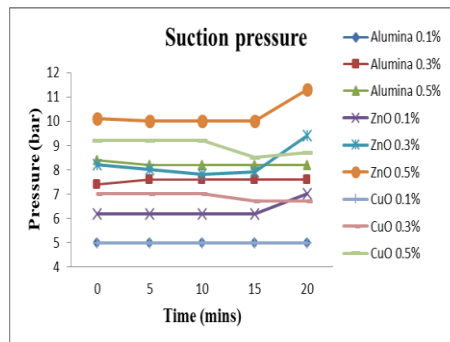


Fig. 12. The suction pressure of Alumina, ZnO, CuO nanoparticle blended R22.

4.2. Effect on suction temperature

The suction temperature of Alumina, Zinc oxide and Copper oxide nanoparticle blended R22 were shown in Fig. 13. In the cooling system condenser full in refrigerant temperature. The coolant is strongly decreasing in temperature relative to nano-coolant in other situations. In the condenser, the enhanced heat transfer rate is due to the presence of nanoparticles in the coolant. Added additional percent of nanofluids raises the suction temperature. The existence of ZnO results in a higher suction temperature.

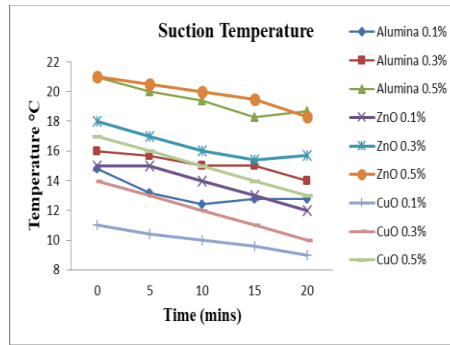


Fig. 13. The suction temperature of Alumina, ZnO, CuO nanoparticle blended R22.

A decreasing trend is observed as the device advances to optimise the addition of nanofluids. For 0.5% addition of nanoparticles, the highest suction temperatures are observed, and for 0.1% addition, the minimum is observed. For Al_2O_3 , ZnO and CuO the maximum nanoparticle suction temperature is 16, 18 and 11° for 0.5% Volume whereas 10, 12 and 8° for 0.1% Volume.

4.3. Effect on discharge pressure

As the volume portion of the nanoparticles in the coolant increases, the discharge pressure varies as shown in Fig. 14. Growing discharge pressure as Al_2O_3 is applied with R22 coolant with an increase in volume concentration. Fluctuations of discharge pressure are observed during the use of ZnO nanoparticle-added coolant R22. During the trial phase, the pressure of the outlet initially declines, then rises and eventually becomes higher. The addition of CuO nanoparticles to the coolant ensures decreased discharge pressure and the lowest pressure is sensed with a 0.5% CuO add-on. For the addition of nanoparticle Al_2O_3 , ZnO and CuO the maximum and minimum discharge pressure is 21.04, 22.13 and 20.41 bar for 0.5% Volume, while 14.49, 14.98 and 14 bar for 0.1% Volume.

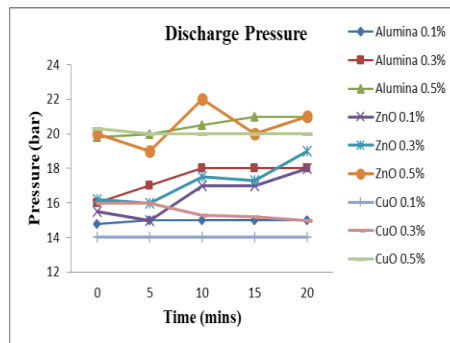


Fig. 14. The discharge pressure of Alumina, ZnO, CuO nanoparticle blended R22.

4.4. Effect on discharge temperature

Fig. 15 shows the discharge temperature of Alumina, Zinc oxide and Copper oxide. With the addition of nanoparticles to the refrigerant, the condenser increases the heat transfer rate, improving the performance of the air conditioning device. Decreases discharge temperature with the addition of nanoparticles [22]. A minimum addition, i.e. 0.1 % Volume of nanoparticles, of 0.5% adds nanoparticles created the minimum release temperature and the minimum discharge temperature. For Al_2O_3 , ZnO and CuO nanomaterial, the maximal release temperature shall be 87, 86 and 85 ° C for 0.1% and the minimum shall be 73, 67 and 64 ° C for 0.5% Volume.

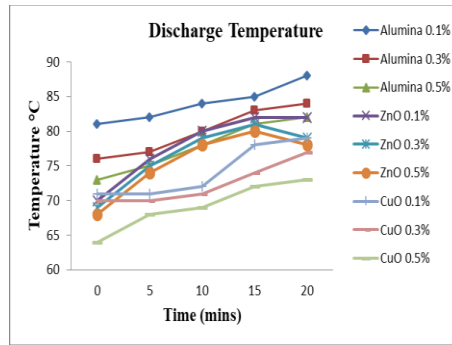


Fig. 15. Discharge temperature of Alumina, ZnO, CuO nanoparticle blended R22.

4.5. Effect on COP

The COP variations for the three nano additives are shown in Fig. 16. The COP rises with the evaporator temperature increasing as the evaporator temperature increases as the cooling potential of the compressor’s power decrease are increased [21]. Amongst other nano additives with COP 5.452 for 0.5 percent CuO is the largest. It’s because of Brown nanocarbon motion in the lubricant more rapidly than the other two. This step alongside nanoparticles increases the coefficient of heat transfer. Comparisons between the three nano additives show, with 0.1 %, 0.3 %, and 0.5 % Volume, that Al₂O₃ nano additive produces lower COP concentrations of 4.613, 4.884 and 5.142. Nano additives can be given in decreasing order based on COP as CuO, ZnO and Al₂O₃. Comparisons of the results with existing works are shown in Table 1.

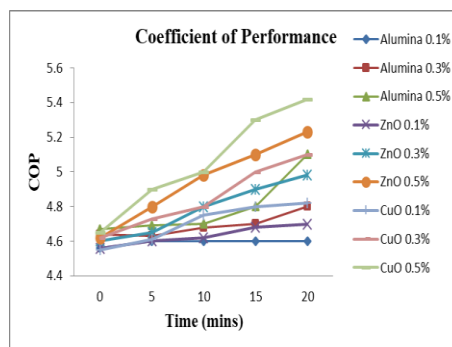


Fig. 16. COP of Alumina, ZnO, CuO nanoparticle blended R22.

Table 1. Comparisons of the results with existing work.

Reference	Alternative refrigerants	Findings	Inferences
[22]	R22	COP summer season 2.3 and winter season 3	Observed that when the cold store air temperature increases
[23]	R22 and R 410 A	The overall COP of the system is 5 to 6% more than R22.	Compared to R22, it has a higher volumetric cooling capacity and has better thermal exchange properties.
[12]	R22 R22 and CuO as nanorefrigerant	COP 9.32 COP 11.51	The addition of nanoadditives facilitates the improvement of cooling capacity.

5. Conclusions

The effects on device output parameters such as suction pressure, suction temperature, discharge pressure and discharge temperature and COP of three nano-additives were studied. Three nanoparticles Al_2O_3 , ZnO and CuO were added to the refrigerant in three different proportions such as 0.1%, 0.3% and 0.5% by volume. A noticeable change in air conditioning system performance is observed with the addition of nanoparticles to the refrigerant.

The highest amount of suction pressure is observed with ZnO, followed by CuO and Alumina. The lowest suction temperature is observed in the order of CuO, ZnO and Alumina. As the system progresses, the suction temperature gets reduced.

The higher discharge pressure is sensed for ZnO nanofluids and lower discharge pressure is sensed for CuO nanofluids. As the system progresses, the discharge pressure of CuO blended refrigerant gets reduced than the other two nanofluids. Hence the compressor efficiency will be better for refrigerant blended with 0.5% of CuO nanofluids.

The decrease in discharge temperature is due to the need to achieve maximum cooling at a higher discharge temperature-COP. With the addition of nanofluids into the refrigerant, discharge temperature decreases for all the type of nanofluids. As the system continues to operate, the lowest discharge temperature is recorded for 0.5% CuO. Higher COP is achieved for 0.5% CuO nanoparticles addition to R22 refrigerant. Inclusion of ZnO nanoparticles into R22 results in lower COP than CuO nanoparticles and least COP was observed with Alumina nanoparticles.

References

- [1] R. Ramesh, R. Vivekananthan, IOSR Journal of Mechanical and Civil Engineering **11**(2), 29 (2014).
- [2] N. Subramani, M. J. Prakash, International Journal of Engineering Science and Technology **3**, 95 (2011).
- [3] V. Siva Reddy, N. L. Panwar, S. C. Kaushik, Clean Technologies and Environmental Policy **14**(1), 47 (2012).
- [4] Vincenzo La Rocca, Giuseppe Panno, Applied Energy **88**(8), 2809 (2011).
- [5] D. H. Yoo, K. S. Hong, H. S. Yang, Thermochemica Acta **455**(1-2), 66 (2007).
- [6] Vedat Oruç, Atilla G. Devecioğlu, International Journal of Refrigeration **55**, 120 (2015).
- [7] O. B. Tsvetkov, Yu. A. Laptev, A. G. Asambaev, International Journal of Thermophysics **17**(3), 597 (1996).
- [8] Dieter Vollath, Nanoparticles - Nanocomposites Nanomaterials - An Introduction for Beginners, Wiley-VCH, Germany, (2013).
- [9] C. H. Shek, J. K. L. Lai, T. S. Gu, G. M. Lin, Nanostructured Materials **8**, 605 (1997).
- [10] D. Sendil Kumar, R. Elansezhian, International Journal of Modern Engineering Research **2**(5), 3390 (2012).
- [11] Angelo Maiorino Rodrigo, Llopis Manuel, Gesù Del Duca, Ciro Aprea, International Journal of Refrigeration **117**, 132 (2020).
- [12] M. Anish, G. Senthil Kumar, N. Beemkumar, B. Kanimozhi, T. Arunkumar, International Journal of Ambient Energy, DOI: 10.1080/01430750.2018.1451376, (2018).
- [13] Aminfar, Habib, and Mohammad Reza Haghgoo, Proceedings of the Institution of Mechanical Engineers, Part C: Journal of Mechanical Engineering Science **227** (1), 100 (2013).
- [14] Shailendra Singh Chauhan, Ritesh Kumar, S. P. S. Rajput, Journal of the Brazilian Society of Mechanical Sciences and Engineering volume **41**, 163 (2019).
- [15] M. Ali, A. A. Shoukat, H. A. Tariq, M. Anwar, H. Ali, Arab. J. Sci. Eng. **44**, 10327 (2019).
- [16] U. Akdag, S. Akcay, D. Demiral, Science **23**, 191 (2019).
- [17] T. M. I. Mahlia, R. Saidur, R, Renewable and Sustainable Energy Reviews **14**, 1888 (2010).
- [18] B. Palaniappan, V. Ramasamy, J. Anal. Calorim. **136**, 223 (2019).

- [19] C. P. Arora, Refrigeration and Air Conditioning, Second edition, Tata McGraw Hill Education (India) Private Limited, New Delhi, (2000).
- [20] G. Liang, I. Mudawar, Int. J. Heat Mass Transf. **136**, 324 (2019).
- [21] M. Mohanraj, International Journal of Thermal Sciences **48**, 1036 (2009).
- [22] C. Aprea, C. Renno, Energy conversion and management **45**(11), 1807 (2008).
- [23] S. S. Jadhav, K. V. Mali, Journal of Mechanical and Civil Engineering, 23 (2017).